COLD SPRING HARBOR
Molecular Case Studies

RESEARCH REPORT

Incidental discovery of acute myeloid leukemia during liquid biopsy of a lung cancer patient

Dingani Nkosi, Caroline A. Miller, Audrey N. Jajosky, and Zoltán N. Oltvai

Department of Pathology and Laboratory Medicine, University of Rochester School of Medicine and Dentistry, Rochester, New York 14642, USA

Abstract Liquid biopsy is considered an alternative to standard next-generation sequencing (NGS) of solid tumor samples when biopsy tissue is inadequate for testing or when testing of a peripheral blood sample is preferred. A common assumption of liquid biopsies is that the NGS data obtained on circulating cell-free DNA is a high-fidelity reflection of what would be found by solid tumor testing. Here, we describe a case that challenges this widely held assumption. A patient diagnosed with lung carcinoma showed pathogenic *IDH1* and *TP53* mutations by liquid biopsy NGS at an outside laboratory. Subsequent in-house NGS of a metastatic lymph node fine-needle aspiration (FNA) sample revealed two pathogenic *EGFR* mutations. Morphologic and immunophenotypic assessment of the patient's blood sample identified acute myeloid leukemia, with in-house NGS confirming and identifying pathogenic *IDH1, TP53*, and *BCOR* mutations, respectively. This case, together with a few similar reports, demonstrates that caution is needed when interpreting liquid biopsy NGS results, especially if they are inconsistent with the presumptive diagnosis. Our case suggests that routine parallel sequencing of peripheral white blood cells would substantially increase the fidelity of the obtained liquid biopsy results.

[Supplemental material is available for this article.]

Corresponding author:
zoltan_oltvai@urmc
.rochester.edu

Ontology terms: acute myeloid leukemia; lung adenocarcinoma

Published by Cold Spring Harbor Laboratory Press

doi:10.1101/mcs.a006201

INTRODUCTION

Genotyping of tumors to detect actionable oncogenic driver mutations and mechanisms of resistance to targeted therapies is standard of care in patients bearing malignancies. For example, epidermal growth factor receptor (*EGFR*) mutations are identified in ~30%–40% of patients with non-small-cell lung cancer (NSCLC). Identification and targeting of *EGFR* mutations have improved progression-free survival in patients with metastatic disease (Rosell et al. 2009; Solomon et al. 2014; Yang et al. 2015; Lindeman et al. 2018).

Tumor tissue is most often used when performing mutation profiling of different cancers. However, in cases in which tumor tissue is limited or exhausted, or when obtaining the tissue is unsafe because of potential patient morbidity, the use of alternative sources of DNA may need to be considered. Cell-free DNA (cfDNA) circulating in peripheral blood can be shed from the primary tumor or metastatic deposits. Several studies in advanced NSCLC have shown high sensitivity in detecting actionable mutations from circulating tumor DNA (ctDNA) (Kuang et al. 2009; Dawson et al. 2013; Newman et al. 2014; Oxnard et al. 2014; Duan et al. 2015; Seki et al. 2018). The noninvasive versus invasive lung evaluation (NILE) prospective, multicenter study revealed that there is no difference in guideline-recommended biomarker detection rate between cfDNA sequencing (27.3%) and tumor tissue

sequencing (21.3%) ($P < 0.0001$ for noninferiority of cfDNA molecular testing) (Leighl et al. 2019). Other prospective studies in patients with NSCLC demonstrate that incorporating liquid biopsy–based genotyping for patient management led to a 15% increase in detection of actionable genomic mutations (Aggarwal et al. 2019; Park et al. 2021). Additionally, previous studies have shown that there is high concordance in *EGFR* mutation detection rate between tissue- and plasma-derived samples (Kuang et al. 2009; Park et al. 2021). Overall, these findings show that liquid biopsies can be utilized in management of patients with advanced NSCLC.

An implicit assumption of liquid biopsies is that the obtained data is a high-fidelity reflection of what would be found by solid tumor next-generation sequencing (NGS) itself. However, the source(s) of circulating cfDNA is inherently unknowable. In older patients with solid tumors, age-related processes such clonal hematopoiesis with oncogenic mutations are common (Acuna-Hidalgo et al. 2017; Park and Bejar 2018), but very rarely second malignancies may also occur. This may complicate the interpretation of liquid biopsy results.

Herein, we describe an elderly patient with NSCLC in whom liquid biopsy-based NGS identified neomorphic *IDH1* p.R132C and truncating *TP53* p.L11fsX mutations. Subsequent in-house NGS performed on a fine-needle aspiration (FNA) sample of a lymph node involved by metastasis only identified two *EGFR* missense mutations, p.G719A and p.S768I. However, NGS performed on the patient's peripheral blood confirmed the *IDH1* and *TP53* mutations and identified an additional *BCOR* p.N1584MfsTer34 mutation, originating from the patient's previously unrecognized acute myeloid leukemia.

RESULTS

Case Presentation

A 68-yr-old otherwise well female presented to her primary care doctor's office for a routine annual visit. Her past medical history was significant for well-controlled sarcoidosis and 20 pack years of smoking. Because of her smoking history she underwent a screening computed tomography (CT) scan and was found to have bilateral pulmonary nodules with the largest being 1.8 cm located in the right middle lobe, and associated lymphadenopathy (Fig. 1A), including subcarinal and stations 4R and 11R positive lymph nodes. Endobronchial ultrasound (EBUS)-guided FNA of a subcarinal lymph node was performed, which showed metastatic carcinoma, favored to be NSCLC (Fig. 1B–G). The patient was immediately referred to medical oncology for further evaluation and management. Her disease was initially clinical stage IIIA (cT1b, cN2, cM0). A solid tumor mutation profiling (STMP) was requested to guide therapy. STMP could not be immediately performed because of a lack of tumor cells on deeper levels of the FNA sample. The treating physician opted to order a liquid biopsy molecular analysis while awaiting repeat EBUS FNA sampling. In addition, the patient was also noted to have mild neutropenia with average cell counts as follows: white cell count, 1.5 K/μL; absolute neutrophil count, 1.1 K/μL; absolute lymphocyte count, 0.4 K/μL; hemoglobin, 12.3 g/dL; and platelet, 303 K/μL. Manual differential showed 5% blasts and 2% reactive lymphocytes.

Liquid Biopsy–Based Testing

Guardant 360 testing, performed by Guardant Health, allows molecular analysis by evaluating cell-free tumor DNA from liquid biopsies in advanced cancers. The Guardant 360 test assesses 74 genes for point mutations (single-nucleotide variants [SNVs]) and insertion/deletion variants (indels), 18 gene amplifications, and six gene fusions by NGS. Guardant Health reported two pathogenic mutation in the submitted blood sample: *IDH1* p.Arg132Cys

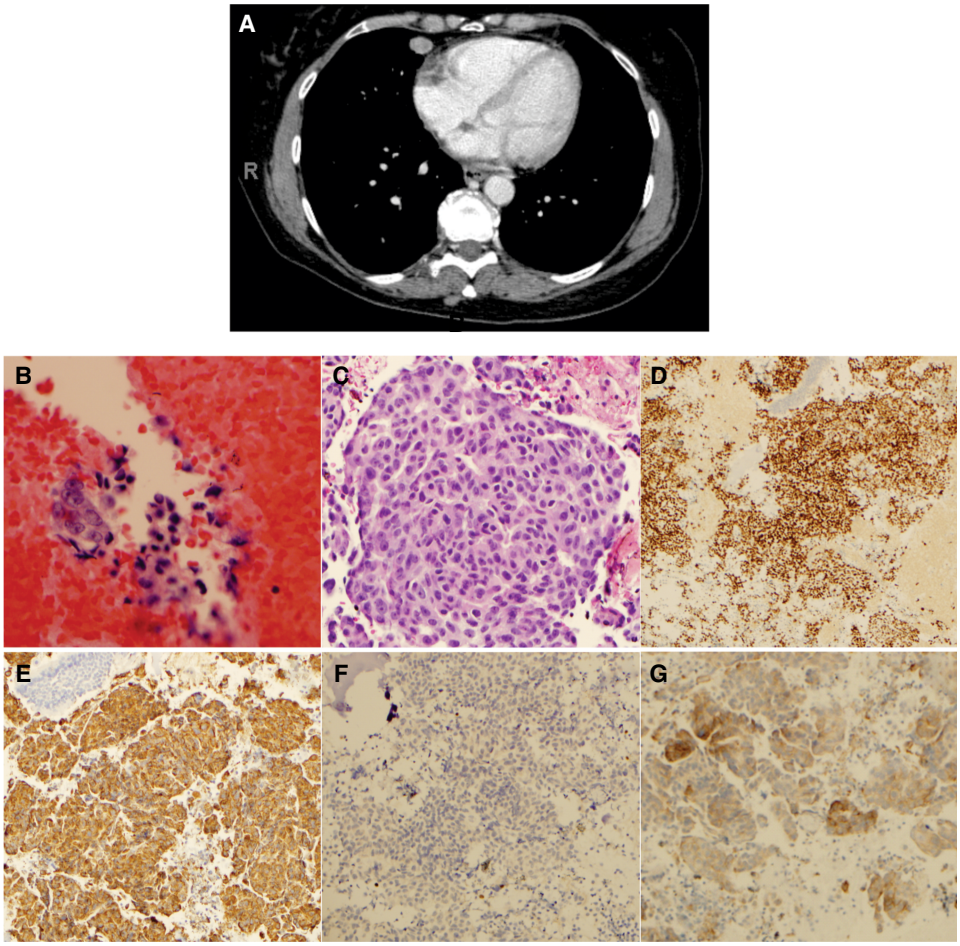

Figure 1. Imaging and morphologic diagnosis of metastatic non-small-cell lung cancer (NSCLC). (*A*) Screening computer tomography (CT) showing a 1.7-cm nodule in the middle lobe of the right lung and multiple additional bilateral subcentimeter pulmonary nodules. (*B–G*) Endobronchial ultrasound (EBUS) fine-needle aspiration (FNA) of lymph nodes positive for metastatic carcinoma, favored to be NSCLC. (*B*) Metastatic carcinoma from subcarinal lymph node sampled at outside institution; (*C*) metastatic carcinoma from a station 4R lymph node sampled at our institution; (*D–G*) immunohistochemical stains performed at our institution on 4R lymph node sample, supporting the diagnosis of NSCLC, more specifically adenocarcinoma (*D*, TTF-1; *E*, Napsin A; *F*, p40; and *G*, PD-L1).

(c.394C > T) with 10.8% cell free DNA and *TP53* p.Leu111fs (c.323_329dup) with 5.5% cell-free DNA (see Table 1). *IDH1* mutations are rare in NSCLC (Rodriguez et al. 2020) and are more commonly associated with hematologic malignancies, whereas *TP53* mutations can be observed in both hematologic malignancies and solid tumors, such as NSCLC (Campling and El-Deiry 2003; Mogi and Kuwano 2011). No *EGFR* or *KRAS* mutations were identified. These results raised the possibility of an alternative or additional diagnosis.

Solid Tumor Next-Generation Sequencing

Subsequently, a new EBUS-guided FNA biopsy of the patient's NSCLC was performed and the obtained tissue was submitted for solid tumor NGS. Solid tumor mutation profiling was done by the ThermoFisher Oncomine focus assay (OFA), which on a DNA level can identify

Table 1. Summary of mutation results identified in the patient by three different next-generation sequencing (NGS) tests

Result 1: Guardant 360	Result 2: STMP OFA	Result 3: Truesight Myeloid
IDH1 p.R132C (c.394C > T) with 10.8% cell-free DNA	*EGFR* p.Gly719Ala (c.2156G > C) at VAF = 42%	*IDH1* p.R132C (c.394C > T) at VAF = 47%
TP53 p.L111fs (c.323_329dup) with 5.5% cell-free DNA	*EGFR* p.Ser768Ile (c.2303G > T) at VAF = 45%	*TP53* p.L111WfsTer12 (c.331delC) at VAF = 85%
		BCOR p.N1584MfsTer34 (c.4751delA) at VAF = 40%

(VAF) Variant allele frequency.

single-nucleotide substitutions and small indels within the mutational hotspots of 35 genes, and copy-number variations in 19 genes. Two pathogenic *EGFR* mutations were detected; p.Gly719Ala (c.2156G > C) at a variant allele frequency (VAF) of 42%; and *EGFR* p.Ser768Ile (c.2303G > T) at VAF of 45% (Table 1). The *EGFR* variants were on different amplicons so we could not determine if they were in *cis* or *trans* (Supplemental Fig. 1). This result was consistent with the morphology-based diagnosis of NSCLC.

Postdiagnosis Course and Second In-House NGS Testing

Three weeks after the lung cancer diagnosis, newer imaging studies showed a right pleural effusion and was now staged as IVA (cT1b, cN2, cM1a). While awaiting the solid tumor panel results, the patient received her first cycle of palliative chemotherapy (pemetrexed and cisplatin), and her persistent neutropenic episodes worsened with average cell counts, as follows: white cell count, 0.5 K/μL; absolute neutrophil count, 0.1 K/μL; absolute lymphocyte count, 0.9 K/μL; hemoglobin, 7.9 g/dL; and platelet, 128 K/μL. Peripheral blood smear review showed 69% circulating blasts (Fig. 2A). Flow cytometry showed blast gate containing 92% of events. These blasts showed expression of CD34, CD38, CD13, HLA-DR (partial, 50%), CD33 (dim, partial), CD117, and CD123 (Supplemental Fig. 2), and 75% of the blasts showed expression of myeloperoxidase (MPO) but were negative for terminal deoxynucleotidyl transferase (TdT) (Fig. 2B) confirming the diagnosis of acute myeloid leukemia (AML).

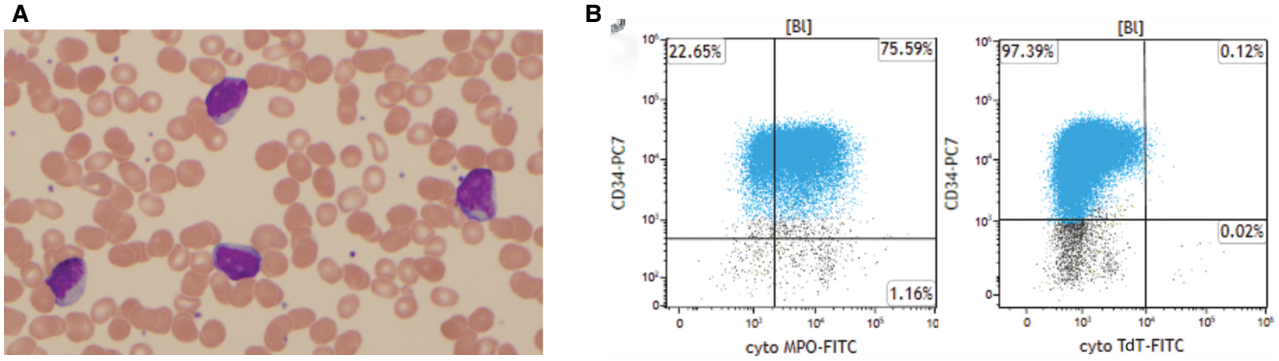

Figure 2. Morphologic and immunophenotypic diagnosis of acute myeloid leukemia. (*A*) Peripheral blood smear showing numerous blasts. (*B*) Flow cytometry immunophenotyping identified a significant blast population expressing CD34, CD38, CD13, HLA-DR (partial, 50%), CD33 (dim, partial), CD117, and CD123 (Supplemental Fig. S2). The majority of $CD34^+$ blasts showed expression of myeloperoxidase (MPO) and lacked expression of terminal deoxynucleotidyl transferase (TdT).

Table 2. Summary of all detected variants

Gene	Chromosome	HGVS DNA reference	HGVS protein reference	Variant type	Predicted effect	dbSNP/dbVar ID
IDH1	Chr 2	NM_005896.4:c.394C > T	NP_005887.2:p.Arg132Cys	SNV	Substitution	rs121913499
TP53	Chr 17	NM_000546.6: c.323_329dup	NP_000537.3:p.Leu111fs	Duplication	Frameshift	rs1131691004
EGFR	Chr 7	NM_005228.5:c.2156G > C	NP_005219.2:p.Gly719Ala	SNV	Substitution	rs121913428
EGFR	Chr 7	NM_005228.5:c.2303G > T	NP_005219.2:p.Ser768Ile	SNV	Substitution	rs121913465
BCOR	Chr X	NM_001123385.1: c.4751delA	NP_001116857:p.N1584MfsTer34	Deletion	Frameshift	
TP53	Chr 17	NM_000546.5: c.331delC	NP_000537.3:p.L111WfsTer12	Deletion	Frameshift	

(SNV) Single-nucleotide variant.

In light of these findings, we performed myeloid neoplasm sequencing on fresh peripheral blood sample on the Illumina Myeloid NGS panel (TruSight Myeloid Sequencing panel). We detected three pathogenic gene mutations: *BCOR* p.N1584MfsTer34 (c.4751delA) at VAF of 40%; *IDH1* p.R132C (c.394C > T) at VAF of 47%; and *TP53* p.L111WfsTer12 (c.331delC) at VAF of 85% (Table 1; Supplemental Fig. 3). Summary of all the variants detected is shown in Table 2. These results were consistent with the Guardant 360 result (*BCOR* gene is not on the Guardant 360 panel).

Karyotyping and fluorescence in situ hybridization (FISH) were also performed on the peripheral blood sample. It revealed trisomy 8 and monosomy 17 in 40% of metaphase spreads, whereas the other 60% showed reciprocal translocation between the long arm of Chromosomes 16 and 21 most compatible with t(16;21)(q24;q22) translocation that would produce a *RUNX1::RUNX1T3* fusion gene. In turn, FISH revealed trisomy 8 (9.5%), abnormal with copy number loss of RARA (17q21) (PML/RARA probe) (93%) and abnormal with one fused RARA (17q21) signal (94%). Summary of the timeline of the key events is shown on Figure 3.

Given the patient's diagnosis of two incurable cancers, treatment for her NSCLC was held and she was started on nonintensive therapy with azacitidine and venetoclax for her AML. A postinduction day 21 bone marrow revealed no evidence of leukemia.

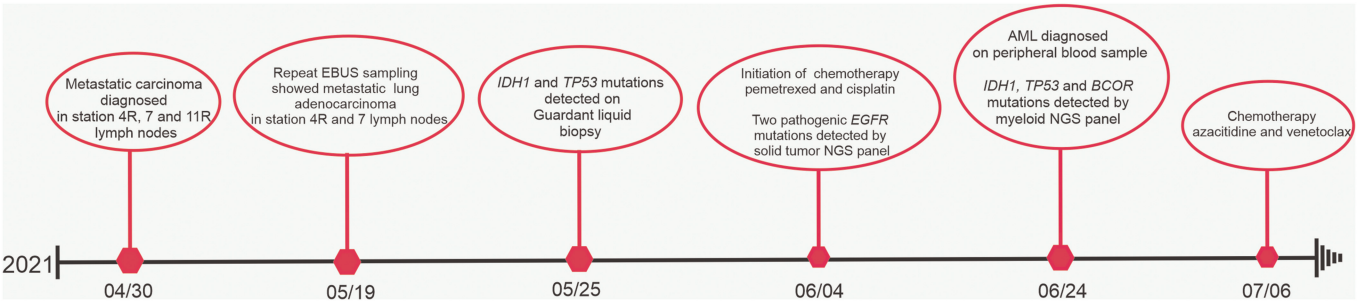

Figure 3. Summary of the timeline with key events. (EBUS) Endobronchial ultrasound, (NGS) next-generation sequencing.

DISCUSSION

Liquid biopsy is considered a good alternative to standard NGS of solid tumor samples when biopsy tissue is inadequate for testing (Alix-Panabières and Pantel 2021; Ignatiadis Sledge and Jeffrey 2021; Martins et al. 2021). The main focus regarding the validity of liquid biopsy results have been on identifying non-tumor-derived clonal hematopoiesis (CH) mutations that can be regarded as biological noise in liquid biopsies (Chan et al. 2020). The most commonly detected mutated genes in CH in healthy individual include *ASXL1, DNMT3A, TET2*, and *TP53*. In contrast, common mutations identified from solid-tumor-related genes such as *KRAS, HRAS, NRAS*, and *PIK3CA* are rarely if ever observed in CH (Park and Bejar 2018; Bolton et al. 2020; Chan et al. 2020). However, some mutations such as those of *TP53* and *IDH1* are commonly seen in AML. Indeed, Razavi et al. (2019) showed that ∼50% of cfDNA mutations identified in cancer patients and 80% from normal healthy controls were characteristic of clonal hematopoiesis (Razavi et al. 2019). These results and others demonstrate the importance of CH mutations in cfDNA genotyping and the role they play in interpreting the variants identified from blood liquid biopsy.

Large population studies have also shown that CH mutations in *IDH1, IDH2*, and *TP53* are associated with increased specificity and development of AML. Specifically, CH mutations with VAF > 10% have been reported to more likely develop hematological malignancies in comparison to those having mutations with lower VAFs (Abelson et al. 2018; Desai et al. 2018). The presence of *IDH1* and *TP53* mutations, both associated with increased risk of AML, together with the *IDH1* VAF of >10%, were suspicious for the presence of current hematologic malignancy rather than CH. Parallel sequencing of leukocyte DNA and cfDNA has been shown to help distinguish between actionable genomic mutations and background noise associated with CH (Hu et al. 2018; Leal et al. 2020; Rose Brannon et al. 2021). Such a practice may assist with immediate identification of the presence of an active hematologic malignancy.

The occurrence of multiple primary malignancies (MPMs) in an individual has a prevalence range of 0.73%–11.7% with synchronous category of MPMs that are diagnosed either simultaneously or >6 mo after the initial primary malignancy considered even less common (Demandante et al. 2003; Liu et al. 2019). Concurrent AML and NSCLC presentation is rare; for example, in a series of 775 AML and 5225 lung cancer cases 12 of them (1.5% of AML cases; 0.23% of lung cancer cases) showed a co-presence of AML and lung cancer (Varadarajan et al. 2009). The absence of *EGFR* mutations in our case also highlights the limitations associated with liquid biopsies. Different malignancies have a subset of common oncogenic driver gene mutations that are specific for that malignancy (Haigis Kevin et al. 2019). The tumor burden and the site of metastatic disease also affect the amount of tumor DNA that can be found in body fluids (Passiglia et al. 2018; Seki et al. 2018). The amount of cfDNA has been shown to be higher in cancer patients than in normal healthy people and further increases with advanced cancer stage (Salvianti et al. 2017; Braig et al. 2019; Herrmann et al. 2019; Martins et al. 2021). Patients with malignancies are associated with higher cfDNA fragmentation (<100 bp) compared to healthy normal individuals, which might hamper analysis (Braig et al. 2019; Martins et al. 2021). However, it is also worth noting that an increase in cfDNA has also been seen in other nonpathological conditions like trauma and surgery (Braig et al. 2019). NSCLC patients with intrathoracic disease, not having spread to distant sites of the body (i.e., stages I–IIIC), may not shed significant DNA into the blood; hence, liquid biopsy–based detection of tumor-associated mutations may be difficult (Seki et al. 2018). Comparison of solid tissue and liquid biopsy sequencing in lung adenocarcinoma patients to identify clinically significant mutations showed that solid tissue sequencing had higher sensitivity (94.8% vs. 52.6%, $P < 0.001$) and accuracy across varied patient

populations including newly diagnosed and treated patients (Lin et al. 2021). This study also showed that some of the clinically relevant mutations between discrepant cases included *EGFR, ALK1*, and *NTRK1* (Lin et al. 2021). Our patient was clinically staged as IIIA and had progressed to stage IVA by the time she started her initial lung cancer treatment. Thus, *EGFR* mutations were most likely masked by the circulating AML cells and therefore could not be amplified.

The clinical application of the liquid biopsies to aid disease diagnosis, profiling, monitoring, and detection of relapse has been limited by low concentrations of circulating cfDNA or circulating tumor cells that are below the levels of analysis (He et al. 2017; Iwama et al. 2017; Palmirotta et al. 2018; Martins et al. 2021). In such unusual but not yet recognized clinical situations interpretation of a negative result is challenging. One of the ways being utilized to solve this challenge is through the use of polymerase chain reaction (PCR)-based technologies such as BEAMing (beads, emulsion, amplification, and magnetic) and droplet digital PCR (ddPCR), which have high sensitivity (range from 1% to 0.001%) (Perakis and Speicher 2017; Palmirotta et al. 2018; Martins et al. 2021). Alternatively, this limitation may be circumvented by automatically reflexing to tumor tissue sample for sequencing to identify any actionable mutations.

This case demonstrates that interpreting liquid biopsy results must be done with care, especially when specific mutations associated with the tumor type are not identified. It also highlights that some of the frequently identified CH-related mutations can be an indication of an underlying but unrelated hematological malignancy. Parallel sequencing of peripheral white blood cells could substantially increase the fidelity of the obtained results (Rose Brannon et al. 2021). Comprehensive workup is required to determine the origin of the identified mutations because of the treatment and prognostic implications.

METHODS

Clinical Specimens

The patient was monitored and/or treated first at an outside institution and then at the University of Rochester Medical Center (URMC) between April 2021 and December 2021. EBUS-guided FNA of subcarinal lymph node and/or peripheral blood samples were collected at various time points of initial URMC assessment.

Specimen Processing and Morphologic Assessment

EBUS-guided FNA specimen was processed by the direct smear method, fixed with 95% ethanol for 15 min prior to processing. The specimens were then processed using the automated tissue processors Leica ASP300S and Leica Peloris II (Leica Biosystems Division of Leica Microsystems Inc.). Three micron-section tissue slides were cut from the processed paraffin blocks and stained with hematoxylin and eosin (H&E) using H&E automated strainers (Sakura Finetek, Inc.; Leica Biosystems, Division of Leica Microsystems Inc.). Immunohistochemical stains were performed as follows: TTF-1 (Agilent), Napsin A (Biocare Medical; Agilent), P40 (Biocare Medical; Leica Biosystems, Division of Leica Microsystems Inc.), and PD-L1 22c3 (Agilent). Morphologic assessment of the H&E-stained FNA biopsy specimens, as well as interpretation of immunohistochemical stains, was performed by a board-certified anatomic pathologist. Wright–Giemsa stain was performed on peripheral blood sample with Midas III Stainer (Fisher Scientific, Part of Thermo Fisher Scientific; Sysmex America, Inc.; Sigma-Aldrich, Inc.). Complete blood count (CBC) was performed on a Sysmex XN-10 Automated Hematology Analyzer (Sysmex America, Inc.) and followed with a manual differential.

Flow Cytometric Immunophenotyping

Immunophenotyping assays were performed by URMC Clinical Flow Cytometry Laboratory for standard clinical care, using a Beckman Coulter Navios Flow Cytometer, FDA approved 10-Color ClearLLab lyophilized immunophenotyping tubes and Kaluza C analysis software (Beckman Coulter Life Sciences). Peripheral blood samples were processed using a stain/lyse/wash protocol. Cell concentrations were adjusted to 3–20 × 10^6/mL to ensure optimal antibody staining and the cells were washed three times before acquisition. Viability was assessed using 7AAD and CD45. Following morphological review of peripheral slide, 10-color analyses were performed for the following surface and cytoplasmic antigens: Kappa, Lambda, CD10, CD5, CD200, CD34, CD38, CD20, CD19, CD45, TCR delta/gamma, CD4, CD2, CD56, CD7, CD8, CD3, CD45, CD16, CD7, CD13, CD64, CD34, CD14, HLA-DR, CD11b, CD15, CD123, CD117, CD33, CD45, 6AC1: cy-TdT, cy-79a, CD22, 6AC2: cy-MPO, CD1a, cy-CD3. Cells were gated to exclude debris (forward scatter versus side scatter and time of flight), to exclude cell doublets (forward scatter height versus forward scatter width), and to isolate leukocyte populations (CD45 versus side scatter). Primary analysis and quality control were performed by the flow cytometry supervisor. Final gating and reporting were performed by a board-certified hematopathologist.

NGS Testing

Genomic DNA was extracted from FNA and peripheral blood samples using the QIAGEN DNeasy blood and tissue kit per the manufacturer's instructions (QIAGEN). Sequencing libraries were prepared for sequencing on the Illumina TruSight Myeloid sequencing panel or on the Thermo Fisher's Oncomine Focus Assay (OFA) panel per the manufacturers' protocols. The enriched DNA libraries were sequenced on an Ion Proton (ThermoFisher, Inc.) (OFA panel) or Illumina MiSeq instruments (version 3 chemistry, 300-base pair [bp] paired-end reads; Illumina) (TruSight Myeloid panel). FASTQ files were processed through vendor-provided bioinformatics pipelines. Variant call files (vcf) were filtered to remove subthreshold calls with less than 500× coverage and/or VAF less than defined, validated thresholds ranging from 1% to 5%, depending on the type of mutation, as follows: 5% for SNVs; 1% for indel mutations <3 bp; and 5% for indel mutations 3 bp or larger. Clinically relevant mutations from this VAF were annotated by a board-certified molecular genetic pathologist (ZNO) manually and reported. Sequenced regions (i.e., mutational hotspot regions, consisting of indicated exons) of the clinically ordered gene set for this patient on the OFA panel were as follows: *AKT1* (NM_001014431.1): 3; *ALK* (NM_004304.4): 21-25; *AR* (NM_000044.3): 6,8; *BRAF* (NM_004333.4): 11,15; *CDK4* (NM_000075.3): 2; *CTNNB1* (NM_001904.3): 3; *DDR2* (NM_006182.2): 5; *EGFR* (NM_005228.3): 3,7,12,15,18-21; *ERBB2* (NM_004448.3): 8,17-22; *ERBB3* (NM_001982.3): 2,3,6,8,9; *ERBB4* (NM_005235.2): 18; *ESR1* (NM_001122740.1): 9; *FGFR2* (NM_000141.4): 7-9,12,14; *FGFR3* (NM_000142.4): 7,9,14,16; *GNA11* (NM_002067.4): 4,5; *GNAQ* (NM_002072.4): 4,5; *HRAS* (NM_001130442.1): 2,3; *IDH1* (NM_005896.3): 4; *IDH2* (NM_002168.2): 4; *JAK1* (NM_002227.2): 14-16; *JAK2* (NM_004972.3): 14; *JAK3* (NM_000215.3): 11,12,15; *KIT* (NM_000222.2): 8,9,11,13,17; *KRAS* (NM_033360.3): 2-4; *MAP2K1* (NM_002755.3): 2,3,6; *MAP2K2* (NM_030662.3): 2; *MET* (NM_001127500.1): 14,16,19; *MTOR* (NM_004958.3): 30,39,40,43,47,53; *NRAS* (NM_002524.4): 2-4; *PDGFRA* (NM_006206.4): 12,14,18; *PIK3CA* (NM_006218.2): 2,5,6,8,10,14,19,21; *RAF1* (NM_002880.3): 7,12; *RET* (NM_020975.4): 10,11,13,15,16; *ROS1* (NM_002944.2): 36,38; *SMO* (NM_005631.4): 4,6,8,9. Sequenced regions (i.e., mutational hotspot regions, consisting of indicated exons) of the clinically ordered gene set for this patient on the TruSight panel were as follows: *ASXL1* (NM_015338.5): 12; *BCOR* (NM_001123385.1): all; *BRAF* (NM_004333.4): 15; *CBL* (NM_005188.3): 8,9; *CSF3R* (NM_156039.3): 14-17; *DNMT3A* (NM_022552.4): all; *ETV6*

(NM_001987.4): all; *EZH2* (NM_004456.4): all; *FBXW7* (NM_033632.3): 9-11; *FLT3* (NM_004119.2): 14,15,20; *GATA1* (NM_002049.3): 2; *GATA2* (NM_032638.4): 2-6; *IDH1* (NM_005896.2): 4; *IDH2* (NM_002168.2): 4; *JAK2* (NM_004972.3): 12,14; *KIT* (NM_000222.2): 2,8-11,13,17; *KRAS* (NM_033360.2): 2,3; *MPL* (NM_005373.2): 10; *MYD88* (NM_002468.4): 3-5; *NOTCH1* (NM_017617.3): 26-28,34; *NPM1* (NM_002520.6): 12; *NRAS* (NM_002524.4): 2,3; *PHF6* (NM_032458.2): all; *PTPN11* (NM_002834.3): 3,13; *RUNX1* (NM_001754.4): all; *SETBP1* (NM_015559.2): 4; *SF3B1* (NM_012433.2): 13-16; *SRSF2* (NM_001195427.1): 1; *STAG2* (NM_001042749.1): all; *TET2* (NM_001127208.2): 3-11; *TP53* (NM_000546.5): 2-11; *U2AF1* (NM_001025203.1): 2,6; *WT1* (NM_024426.4): 7,9; *ZRSR2* (NM_005089.3): all.

ADDITIONAL INFORMATION

Data Deposition and Access

The consent documentation signed by the patient does not expressly allow submission of full sequencing data (FASTQ, BAM/BAI, VCF) to external data repositories. The interpreted variants were submitted to ClinVar (https://www.ncbi.nlm.nih.gov/clinvar/) and can be found under accession numbers SCV002506981–SCV002506986.

Ethics Statement

The patient signed the institution-approved, standard consent for clinical diagnostic testing by NGS, including agreement to the opt-in/-out clause for use of genetic and other diagnostic information for research purposes. This consent mechanism does not allow for sharing of genetic and other diagnostic information beyond that clinically relevant and reported in the manuscript.

Competing Interest Statement

The authors have declared no competing interest.

Referees

Susan E. Harley
Anonymous

Received February 8, 2022; accepted in revised form April 25, 2022.

Acknowledgments

We thank Tia LaBarge and Sierra Kovar (University of Rochester Medical Center) and the Reviewers for their comments on the manuscript.

Author Contributions

D.N. and C.A.M. reviewed and analyzed the data, created the figures, and wrote the manuscript with input from A.N.J. and Z.N.O. All authors read the manuscript and approved its final version.

REFERENCES

Abelson S, Collord G, Ng SWK, Weissbrod O, Mendelson Cohen N, Niemeyer E, Barda N, Zuzarte PC, Heisler L, Sundaravadanam Y, et al. 2018. Prediction of acute myeloid leukaemia risk in healthy individuals. *Nature* **559:** 400–404. doi:10.1038/s41586-018-0317-6

Acuna-Hidalgo R, Sengul H, Steehouwer M, van de Vorst M, Vermeulen SH, Kiemeney LALM, Veltman JA, Gilissen C, Hoischen A. 2017. Ultra-sensitive sequencing identifies high prevalence of clonal hematopoiesis-associated mutations throughout adult life. *Am J Hum Genet* **101:** 50–64. doi:10.1016/j.ajhg.2017.05.013

Aggarwal C, Thompson JC, Black TA, Katz SI, Fan R, Yee SS, Chien AL, Evans TL, Bauml JM, Alley EW, et al. 2019. Clinical implications of plasma-based genotyping with the delivery of personalized therapy in metastatic non–small cell lung cancer. *JAMA Oncol* **5:** 173–180. doi:10.1001/jamaoncol.2018.4305

Alix-Panabières C, Pantel K. 2021. Liquid biopsy: from discovery to clinical implementation. *Mol Oncol* **15:** 1617–1621. doi:10.1002/1878-0261.12997

Bolton KL, Ptashkin RN, Gao T, Braunstein L, Devlin SM, Kelly D, Patel M, Berthon A, Syed A, Yabe M, et al. 2020. Cancer therapy shapes the fitness landscape of clonal hematopoiesis. *Nat Genet* **52:** 1219–1226. doi:10.1038/s41588-020-00710-0

Braig D, Becherer C, Bickert C, Braig M, Claus R, Eisenhardt AE, Heinz J, Scholber J, Herget GW, Bronsert P, et al. 2019. Genotyping of circulating cell-free DNA enables noninvasive tumor detection in myxoid liposarcomas. *Int J Cancer* **145:** 1148–1161. doi:10.1002/ijc.32216

Campling BG, El-Deiry WS. 2003. Clinical implication of p53 mutation in lung cancer. *Mol Biotechnol* **24:** 141–156. doi:10.1385/MB:24:2:141

Chan HT, Chin YM, Nakamura Y, Low S-K. 2020. Clonal hematopoiesis in liquid biopsy: from biological noise to valuable clinical implications. *Cancers (Basel)* **12:** 2277. doi:10.3390/cancers12082277

Dawson SJ, Tsui DW, Murtaza M, Biggs H, Rueda OM, Chin SF, Dunning MJ, Gale D, Forshew T, Mahler-Araujo B, et al. 2013. Analysis of circulating tumor DNA to monitor metastatic breast cancer. *N Engl J Med* **368:** 1199–1209. doi:10.1056/NEJMoa1213261

Demandante CGN, Troyer DA, Miles TP. 2003. Multiple primary malignant neoplasms: case report and a comprehensive review of the literature. *Am J Clin Oncol* **26:** 79–83. doi:10.1097/00000421-200302000-00015

Desai P, Mencia-Trinchant N, Savenkov O, Simon MS, Cheang G, Lee S, Samuel M, Ritchie EK, Guzman ML, Ballman KV, et al. 2018. Somatic mutations precede acute myeloid leukemia years before diagnosis. *Nat Med* **24:** 1015–1023. doi:10.1038/s41591-018-0081-z

Duan H, Lu J, Lu T, Gao J, Zhang J, Xu Y, Wang M, Wu H, Liang Z, Liu T. 2015. Comparison of EGFR mutation status between plasma and tumor tissue in non–small cell lung cancer using the Scorpion ARMS method and the possible prognostic significance of plasma *EGFR* mutation status. *Int J Clin Exp Pathol* **8:** 13136–13145.

Haigis Kevin M, Cichowski K, Elledge Stephen J. 2019. Tissue-specificity in cancer: the rule, not the exception. *Science* **363:** 1150–1151. doi:10.1126/science.aaw3472

He J, Tan W, Ma J. 2017. Circulating tumor cells and DNA for real-time EGFR detection and monitoring of non-small-cell lung cancer. *Future Oncol* **13:** 787–797. doi:10.2217/fon-2016-0427

Herrmann S, Zhan T, Betge J, Rauscher B, Belle S, Gutting T, Schulte N, Jesenofsky R, Härtel N, Gaiser T, et al. 2019. Detection of mutational patterns in cell-free DNA of colorectal cancer by custom amplicon sequencing. *Mol Oncol* **13:** 1669–1683. doi:10.1002/1878-0261.12539

Hu Y, Ulrich BC, Supplee J, Kuang Y, Lizotte PH, Feeney NB, Guibert NM, Awad MM, Wong KK, Jänne PA, et al. 2018. False-positive plasma genotyping due to clonal hematopoiesis. *Clin Cancer Res* **24:** 4437. doi:10.1158/1078-0432.CCR-18-0143

Ignatiadis M, Sledge GW, Jeffrey SS. 2021. Liquid biopsy enters the clinic: implementation issues and future challenges. *Nat Rev Clin Oncol* **18:** 297–312. doi:10.1038/s41571-020-00457-x

Iwama E, Sakai K, Azuma K, Harada T, Harada D, Nosaki K, Hotta K, Ohyanagi F, Kurata T, Fukuhara T, et al. 2017. Monitoring of somatic mutations in circulating cell-free DNA by digital PCR and next-generation sequencing during afatinib treatment in patients with lung adenocarcinoma positive for EGFR activating mutations. *Ann Oncol* **28:** 136–141. doi:10.1093/annonc/mdw531

Kuang Y, Rogers A, Yeap BY, Wang L, Makrigiorgos M, Vetrand K, Thiede S, Distel RJ, Jänne PA. 2009. Noninvasive detection of *EGFR* T790M in gefitinib or erlotinib resistant non–small cell lung cancer. *Clin Cancer Res* **15:** 2630. doi:10.1158/1078-0432.CCR-08-2592

Leal A, van Grieken NCT, Palsgrove DN, Phallen J, Medina JE, Hruban C, Broeckaert MAM, Anagnostou V, Adleff V, Bruhm DC, et al. 2020. White blood cell and cell-free DNA analyses for detection of residual disease in gastric cancer. *Nat Commun* **11:** 525. doi:10.1038/s41467-020-14310-3

Leighl NB, Page RD, Raymond VM, Daniel DB, Divers SG, Reckamp KL, Villalona-Calero MA, Dix D, Odegaard JI, Lanman RB, et al. 2019. Clinical utility of comprehensive cell-free DNA analysis to identify genomic biomarkers in patients with newly diagnosed metastatic non–small cell lung cancer. *Clin Cancer Res* **25:** 4691. doi:10.1158/1078-0432.CCR-19-0624

Lin LH, Allison DHR, Feng Y, Jour G, Park K, Zhou F, Moreira AL, Shen G, Feng X, Sabari J, et al. 2021. Comparison of solid tissue sequencing and liquid biopsy accuracy in identification of clinically relevant gene mutations and rearrangements in lung adenocarcinomas. *Mod Pathol* **34:** 2168–2174. doi:10.1038/s41379-021-00880-0

Lindeman NI, Cagle PT, Aisner DL, Arcila ME, Beasley MB, Bernicker EH, Colasacco C, Dacic S, Hirsch FR, Kerr K, et al. 2018. Updated molecular testing guideline for the selection of lung cancer patients for treatment with targeted tyrosine kinase inhibitors: guideline from the College of American Pathologists, the International Association for the Study of Lung Cancer, and the Association for Molecular Pathology. *Arch Pathol Lab Med* **142:** 321–346. doi:10.5858/arpa.2017-0388-CP

Liu S, Wei X, Xiong Y, Mi R, Yin Q. 2019. Thirty-two case reports of synchronous hematological malignancy and solid tumor. *Turk J Haematol* **36:** 291–294. doi:10.4274/tjh.galenos.2019.2019.0071

Martins I, Ribeiro IP, Jorge J, Gonçalves AC, Sarmento-Ribeiro AB, Melo JB, Carreira IM. 2021. Liquid biopsies: applications for cancer diagnosis and monitoring. *Genes (Basel)* **12:** 349. doi:10.3390/genes12030349

Mogi A, Kuwano H. 2011. TP53 mutations in non–small cell lung cancer. *J Biomed Biotechnol* **2011:** 583929. doi:10.1155/2011/583929

Newman AM, Bratman SV, To J, Wynne JF, Eclov NC, Modlin LA, Liu CL, Neal JW, Wakelee HA, Merritt RE, et al. 2014. An ultrasensitive method for quantitating circulating tumor DNA with broad patient coverage. *Nat Med* **20:** 548–554. doi:10.1038/nm.3519

Oxnard GR, Paweletz CP, Kuang Y, Mach SL, O'Connell A, Messineo MM, Luke JJ, Butaney M, Kirschmeier P, Jackman DM, et al. 2014. Noninvasive detection of response and resistance in *EGFR*-mutant lung cancer using quantitative next-generation genotyping of cell-free plasma DNA. *Clin Cancer Res* **20:** 1698. doi:10.1158/1078-0432.CCR-13-2482

Palmirotta R, Lovero D, Cafforio P, Felici C, Mannavola F, Pellè E, Quaresmini D, Tucci M, Silvestris F. 2018. Liquid biopsy of cancer: a multimodal diagnostic tool in clinical oncology. *Ther Adv Med Oncol* **10:** 1758835918794630. doi:10.1177/1758835918794630

Park S, Bejar R. 2018. Clonal hematopoiesis in aging. *Curr Stem Cell Rep* **4:** 209–219. doi:10.1007/s40778-018-0133-9

Park S, Olsen S, Ku BM, Lee MS, Jung HA, Sun JM, Lee SH, Ahn JS, Park K, Choi YL, et al. 2021. High concordance of actionable genomic alterations identified between circulating tumor DNA–based and tissue-based next-generation sequencing testing in advanced non–small cell lung cancer: the Korean Lung Liquid Versus Invasive Biopsy Program. *Cancer* **127:** 3019–3028. doi:10.1002/cncr.33571

Passiglia F, Rizzo S, Di Maio M, Galvano A, Badalamenti G, Listì A, Gulotta L, Castiglia M, Fulfaro F, Bazan V, et al. 2018. The diagnostic accuracy of circulating tumor DNA for the detection of *EGFR*-T790M mutation in NSCLC: a systematic review and meta-analysis. *Sci Rep* **8:** 13379. doi:10.1038/s41598-018-30780-4

Perakis S, Speicher MR. 2017. Emerging concepts in liquid biopsies. *BMC Med* **15:** 75. doi:10.1186/s12916-017-0840-6

Razavi P, Li BT, Brown DN, Jung B, Hubbell E, Shen R, Abida W, Juluru K, De Bruijn I, Hou C, et al. 2019. High-intensity sequencing reveals the sources of plasma circulating cell-free DNA variants. *Nat Med* **25:** 1928–1937. doi:10.1038/s41591-019-0652-7

Rodriguez EF, De Marchi F, Lokhandwala PM, Belchis D, Xian R, Gocke CD, Eshleman JR, Illei P, Li MT. 2020. *IDH1* and *IDH2* mutations in lung adenocarcinomas: evidences of subclonal evolution. *Cancer Med* **9:** 4386–4394. doi:10.1002/cam4.3058

Rose Brannon A, Jayakumaran G, Diosdado M, Patel J, Razumova A, Hu Y, Meng F, Haque M, Sadowska J, Murphy BJ, et al. 2021. Enhanced specificity of clinical high-sensitivity tumor mutation profiling in cell-free DNA via paired normal sequencing using MSK-ACCESS. *Nat Commun* **12:** 3770. doi:10.1038/s41467-021-24109-5

Rosell R, Moran T, Queralt C, Porta R, Cardenal F, Camps C, Majem M, Lopez-Vivanco G, Isla D, Provencio M, et al. 2009. Screening for epidermal growth factor receptor mutations in lung cancer. *N Engl J Med* **361:** 958–967. doi:10.1056/NEJMoa0904554

Salvianti F, Giuliani C, Petrone L, Mancini I, Vezzosi V, Pupilli C, Pinzani P. 2017. Integrity and quantity of total cell-free DNA in the diagnosis of thyroid cancer: correlation with cytological classification. *Int J Mol Sci* **18:** 1350. doi:10.3390/ijms18071350

Seki Y, Fujiwara Y, Kohno T, Yoshida K, Goto Y, Horinouchi H, Kanda S, Nokihara H, Yamamoto N, Kuwano K, et al. 2018. Circulating cell-free plasma tumour DNA shows a higher incidence of *EGFR* mutations in patients with extrathoracic disease progression. *ESMO Open* **3:** e000292. doi:10.1136/esmoopen-2017-000292

Solomon BJ, Mok T, Kim DW, Wu YL, Nakagawa K, Mekhail T, Felip E, Cappuzzo F, Paolini J, Usari T, et al. 2014. First-line crizotinib versus chemotherapy in ALK-positive lung cancer. *N Engl J Med* **371:** 2167–2177. doi:10.1056/NEJMoa1408440

Varadarajan R, Ford L, Sait SN, Block AW, Barcos M, Wallace PK, Ramnath N, Wang ES, Wetzler M. 2009. Metachronous and synchronous presentation of acute myeloid leukemia and lung cancer. *Leuk Res* **33:** 1208–1211. doi:10.1016/j.leukres.2008.12.016

Yang JC, Wu YL, Schuler M, Sebastian M, Popat S, Yamamoto N, Zhou C, Hu CP, O'Byrne K, Feng J, et al. 2015. Afatinib versus cisplatin-based chemotherapy for *EGFR* mutation–positive lung adenocarcinoma (LUX-Lung 3 and LUX-Lung 6): analysis of overall survival data from two randomised, phase 3 trials. *Lancet Oncol* **16:** 141–151. doi:10.1016/S1470-2045(14)71173-8